GLOBAL THREE-DIMENSIONAL SIMULATION AND RADIATIVE FORCING OF VARIOUS AEROSOL SPECIES

* Toshihiko Takemura [1], Hajime Okamoto [2], Atusi Numaguti [3], Akiko Higurashi [4], and Teruyuki Nakajima [1]

[1] Center for Climate System Research, University of Tokyo, Tokyo, Japan
[2] Kashima Space Research Center, Communications Research Laboratory, Ibaraki, Japan
[3] Graduate School of Environmental Earth Science, Hokkaido University, Hokkaido, Japan
[4] National Institute for Environmental Studies, Tsukuba, Japan

ABSTRACT

A global three-dimensional model that can treat various species of aerosols in the atmosphere is developed using a framework of Atmospheric General Circulation Model (AGCM). Main aerosols in the troposphere, i.e., soil dust, carbonaceous (organic and black carbon), sulfate, and sea-salt aerosols, are introduced into this model. To evaluate aerosol effects on the climate system and to compare simulated results with observations, the optical thickness and the radiative forcing by aerosol direct effect are also calculated taking into account the size distribution, optical properties of each aerosol species, and changes of the particle radius depending on the relative humidity. The model results are validated using not only measured surface and vertical aerosol concentrations but also retrieved aerosol optical parameters from NOAA/AVHRR and AERONET. A general agreement is found between the simulated result with the observation globally, seasonally and quantitatively. Aerosol direct radiative forcing is negative for sulfate and sea-salt aerosols, on the other hand, it is possible to be both positive and negative for soil dust and carbonaceous aerosols depending on the particle size, surface albedo, altitudes of cloud and aerosol layers, and internal mixing with water.

* Corresponding author address: Toshihiko Takemura, Center for Climate System Research, University of Tokyo, 4-6-1 Komaba, Meguro-ku, Tokyo 153-8904, Japan; e-mail: toshi@ccsr.u-tokyo.ac.jp

1. INTRODUCTION

It is important to estimate the climate forcing by anthropogenic and natural aerosols for predicting the future climate change. There is, however, large uncertainty of the estimate for aerosol radiative forcing. According to IPCC (1996), the radiative forcing of anthropogenic greenhouse gases is estimated as 2.45 W m^{-2} with an uncertainty of 15 %, while the total direct aerosol forcing is estimated to be -0.5 W m^{-2} with a large uncertainty of a factor of 2. Moreover, the total indirect forcing was estimated to be in a wider range from 0 to -1.5 W m^{-2} because the cloud-aerosol interaction process itself has been scarcely understood. In order to minimize these uncertainties, an adequate aerosol transport model is necessary to be developed for simulating the aerosol distribution of various species. But past studies concerning aerosol transport modeling mostly treated one kind of aerosol, so they were able to be compared using only *in situ* measurements of aerosol concentrations at some locations. But in situ measurements are limited and include local variance, so that it is difficult to obtain a proper validation for such aerosol transport

models on global scale. In recent years, on the other hand, large amounts of satellite products for aerosols have become available by the new progress in remote sensing technologies. For example, Higurashi and Nakajima (1999) analyzed the global distribution of the aerosol optical thickness and the Ångström exponent over ocean retrieved from two channels of NOAA/AVHRR. There is also Aerosol Robotic Network (AERONET) that is observational network of aerosol optical properties over land using multi-channels.

Therefore we develop a global three-dimensional model that can treat main aerosol species in the troposphere (soil dust, carbonaceous (organic and black carbon), sulfate, and sea-salt) in this study. Then simulated results are compared with not only measured surface aerosol concentrations but also the AVHRR and AERONET optical thickness, i.e., observed column loading. The direct radiative forcing for four aerosol species is also estimated by the link with the transport model.

2. MODEL DESCRIPTION

The present three-dimensional aerosol model is coupled with CCSR (Center for Climate System Research) / NIES (National Institute for Environmental Studies) AGCM. Resolution is T21 (triangular truncation with wavenumber 21, i.e., about 5.6° longitude by 5.6° latitude) and 11 layers (sigma levels at 0.995, 0.980, 0.950, 0.900, 0.815, 0.679, 0.513, 0.348, 0.203, 0.092, and 0.021). The basic features of CCSR/NIES AGCM are found in Numaguti (1993), and newly implemented physical processes are discussed in Numaguti et al. (1995). This AGCM adopts a radiation scheme based on the k-distribution and the two-stream discrete ordinate method (Nakajima and Tanaka 1986; Nakajima et al. 2000).

Various physical processes of the emission, advection, diffusion, wet deposition (sub- and in-cloud scavenging), dry deposition, and gravitational settling are newly introduced into this transport model. It is possible to select whether wind and temperature fields are nudged by NCEP/NCAR reanalysis data or not. The nudged field is used for the results shown in this paper. The wind velocity with an altitude of 10-m is calculated for the emission of soil dust and sea-salt aerosols based on the Monin-Obukhov similarity theory in consideration for the unstable condition of the atmosphere. GEIA (Global Emissions Inventory Activities) and FAO (Food and Agriculture Organization of the United Nations) database are used for estimations of emission fluxes of carbonaceous and sulfur species. Emission sources for carbonaceous aerosols are six categories; forest fires in tropical rain forests, those in other forests, fossil fuel consumption, fuel wood consumption, combustion of agricultural wastes, and gas to particle conversion of terpene emitted from plants. Carbonaceous aerosols are treated as the internal mixture of black carbon and organic carbon in this model. Chemical reactions of precursor gases, such as sulfur dioxide and dimethylsulfide (DMS), are treated for sulfate aerosols. Sulfur dioxide is emitted from fossil fuel consumption and volcanoes, and DMS is emitted from the oceanic phytoplankton in this model. We also calculate the optical thickness and direct radiative forcing considering size distributions, changes of the particle radius depending on the relative humidity, and differences of the extinction efficiency among each aerosol type. The detailed description for the present model can be seen in Takemura et al. (1999).

3. GLOBAL DISTRIBUTION OF AEROSOL OPTICAL THICKNESS

Figure 1 shows the simulated distributions of the combined monthly mean optical thickness of soil dust, carbonaceous, sulfate, and sea-salt aerosols in January, April, July, and October. The most prominent contributors to the total optical thick-

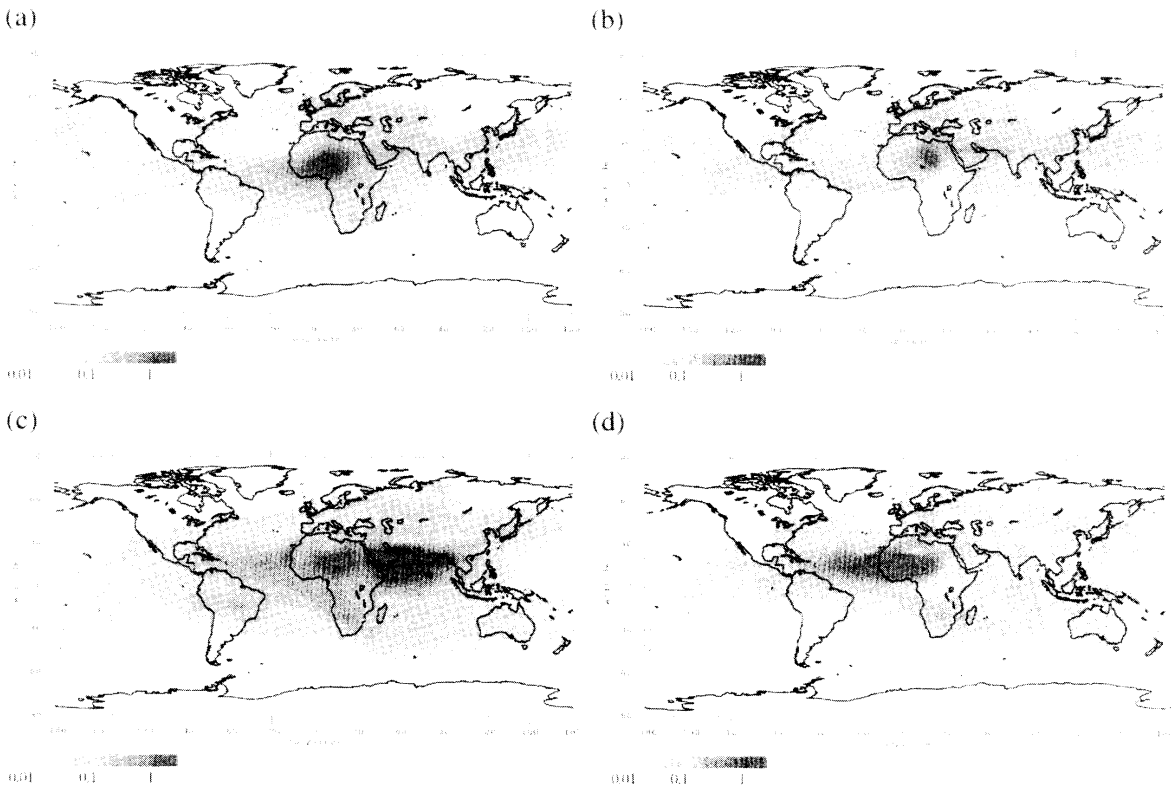

Figure 1. Monthly mean distributions of the simulated optical thickness for a mixed state of four aerosol species (soil dust, carbonaceous (black and organic carbon), sulfate, and sea-salt) at a wavelength of 0.55 μm in (a) January, (b) April, (c) July, and (d) October.

ness are soil dust and carbonaceous aerosols. Saharan dust particles are transported by the trade wind over the North Atlantic throughout the year. Large amount of soil dust is also seen around the Arabian Sea in the Northern Hemisphere summer, which can be explained by the strong monsoon wind in this season. Carbonaceous aerosols originating from biomass burning are remarkable over Central Africa in January and over South Africa and Amazon in July. In the mid-latitudes of the Northern Hemisphere, anthropogenic carbonaceous and sulfate aerosols prevail noticeably showing distinct seasonal variation with the large optical thickness in summer. These geographical patterns and seasonal variabilities of the optical thickness were detected by AVHRR retrievals (Nakajima and Higurashi 1998; Higurashi et al. 1999).

Figure 2 shows an example of the simulated optical thickness for each aerosol type and a mixture of four aerosol species with the corresponding AVHRR retrievals. The simulated optical thickness is a little smaller than the AVHRR one over industrial regions (Mediterranean Sea and Japan). One of the significant results is that the simulated relative contribution of anthropogenic carbonaceous aerosols to the total optical thickness is relatively large at mid-latitudes of the Northern Hemisphere, which agrees with recent observations. This result leads to a conclusion that the radiative effect evaluation of aerosols on the climate system is necessary to be modified because optical properties of carbonaceous aerosols are different from those of sulfate aerosols, which have been considered to the dominant anthropogenic aerosols. On the other hand, the simulated soil dust aerosols are a little overestimated from July to October over the Gulf of Guinea. The small-scale convection, which is difficult to be modeled in the general cir-

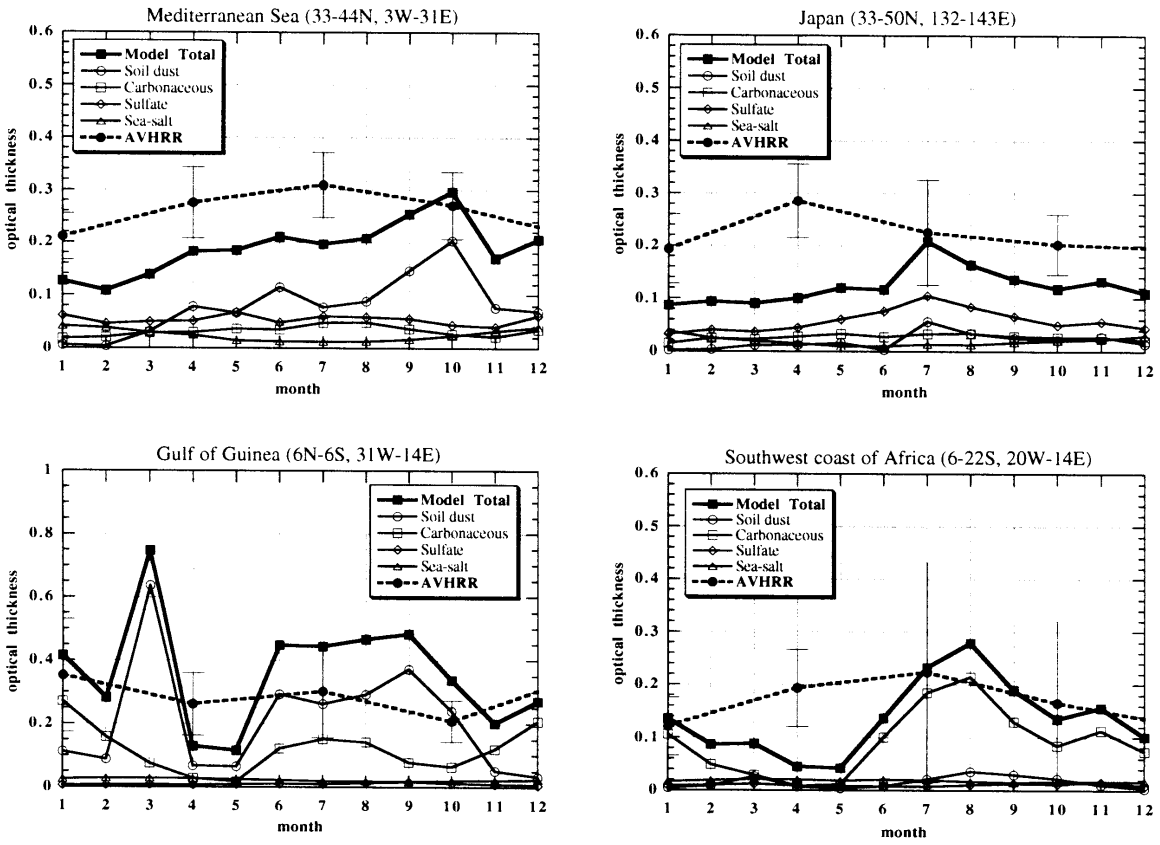

Figure 2. Seasonal variation of simulated and AVHRR retrieved optical thicknesses. The simulated optical thickness is shown for a mixed state of four aerosol species (solid lines with filled symbols) and each aerosol type (solid lines with opaque symbols), and AVHRR retrieved one (dashed lines) is also shown with the standard deviation.

culation model, may be very effective in generating dust storms. The simulated optical thickness is, however, close to AVHRR retrievals in the biomass burning season of the Southern Hemisphere (over the southwest coast of Africa). Figure 3 shows the same comparison as Figure 2 but with the AERONET observation. Over the industrial region (Ispra), the simulated optical thickness is a little underestimated, while it is good agreement with the AERONET one (~0.1) over the remote ocean (Bermuda). There are some differences between the simulated and AERONET optical thicknesses in Barbados and South Africa (Mongu), but the year of NCEP/NCAR reanalysis data using on the nudging is different from that of observations.

Satellite observations such as AVHRR detected that the latitude of the maximum optical thickness shifts seasonally off the west coast of North Africa, that is around 10°N in January, on the other hand, 20°N in July. This seasonal shift is reproduced well with the proper optical thickness in this model (Figure 4). The simulated result suggests that soil dust from the Sahara Desert and carbonaceous aerosols from biomass burning over Central Africa coexist in January over the tropical North Atlantic.

The simulated aerosol column loading is much variable depending on the in-cloud scavenging. It is, therefore, necessary not only to study microphysical properties of cloud-aerosol interaction in

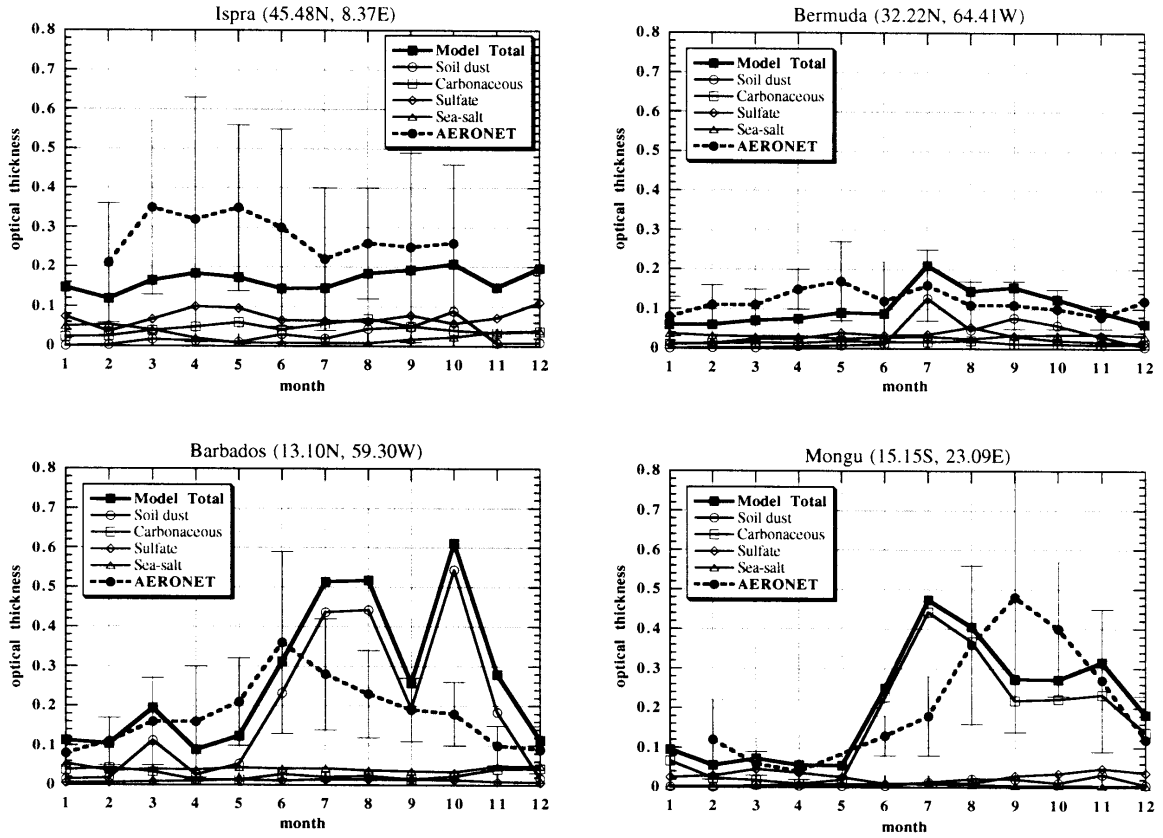

Figure 3. Same as Figure 2 but for simulated and AERONET optical thicknesses.

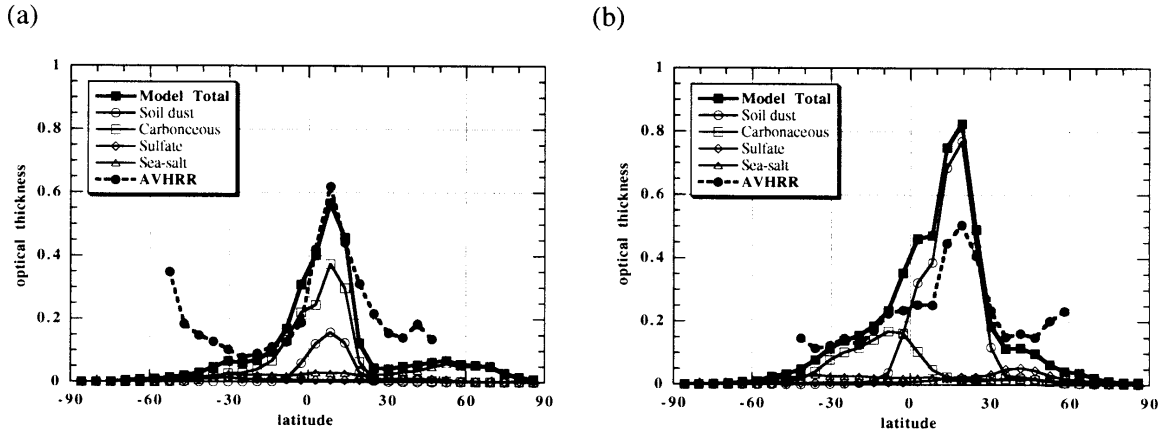

Figure 4. Comparison between simulated (solid lines) and AVHRR (dashed lines) optical thicknesses along 22.5°W in (a) January and (b) July.

more detail but also to observe liquid and ice water content including vertical distributions globally, so it is hoped that the spaceborne cloud radar will play an important role.

4. RADIATIVE FORCING FOR AEROSOL DIRECT EFFECT

Figure 5 shows the annual mean distribution of the direct radiative forcing for each aerosol species at the tropopause for clear-sky. Though soil dust aerosols have positive forcing at most regions, the strength and sign of the radiative forcing are much variable depending on the size distribution and the aerosol vertical profile according to sensitivity tests. Carbonaceous aerosols from biomass burning have the strong negative forcing for clear-sky, while they have the positive one over deserts and Tibet because of the large surface albedo. The radiative forcing of sulfate aerosols is negative strongly over industrial regions, and sea-salt aerosols also have negative forcing relatively homogeneous over ocean.

On the other hand, Figure 6 shows the same as Figure 5 but for including cloudy-sky. Radiative forcings of soil dust and carbonaceous aerosols shift more positive than that for clear-sky. This may be because soil dust and black carbon strongly absorb the multi-scattering radiation affected by cloud layers, so it is important to obtain the information for vertical profiles of aerosol particles. The spaceborne lidar is, therefore, an effective tool to estimate proper aerosol radiative forcing.

5. CONCLUSION

The three-dimensional global aerosol model that can treat main aerosol species in the troposphere has been developed, so that it has become possible to validate it using satellite data, i.e., AVHRR retrievals, and ground-based optical observations of AERONET. Comparison of the simulated optical thickness for a mixed state of major four aerosol species with optical observations have found a general agreement globally, seasonally, and quantitatively. The simulated relative contribution of anthropogenic carbonaceous aerosols to the total optical thickness in mid-latitudes of the Northern Hemisphere is larger than that have ever been considered, which agrees with recent observations. The results have also suggested that the seasonal shift of the aerosol optical thickness peak off the west coast of North Africa is caused by a coexistence of not only soil dust but also carbonaceous aerosols. The direct radiative forcing is negative for sulfate and sea-salt aerosols, on the other hand, it can be both positive and negative for absorbing aerosols, such as soil dust and black carbon, depending on not only particle size distributions, surface albedo, and structures of internal mixture but also vertical profiles of aerosols and clouds. The spaceborne radar and lidar are, therefore, effective for validations of the global aerosol transport model.

The main future works are as follows: an analysis of the feedback effect of aerosol distributions to the atmospheric and radiative field; estimation of indirect radiative forcing; estimation of future radiative forcing considering the emission scenario.

References

Higurashi, A., and T. Nakajima, 1999: Development of a two-channel aerosol retrieval algorithm on a global scale using NOAA AVHRR. *J. Atmos. Sci.*, **56**, 924-941.

Higurashi, A., T. Nakajima, B. N. Holben, A. Smirnov, R. Frouin, and B. Chatenet, 1999: A study of global aerosol optical climatology with two channel AVHRR remote sensing. *J. Climate*, in press.

IPCC (the International Panel on Climate Change), 1996: *Climate Change 1995: The Science of Climate Change*. J. T. Houghton, L. G. Meira Filho, B. A. Callander, N. Harris, A. Kattenberg, and K. Maskell (Eds.), 572 pp., Cambridge

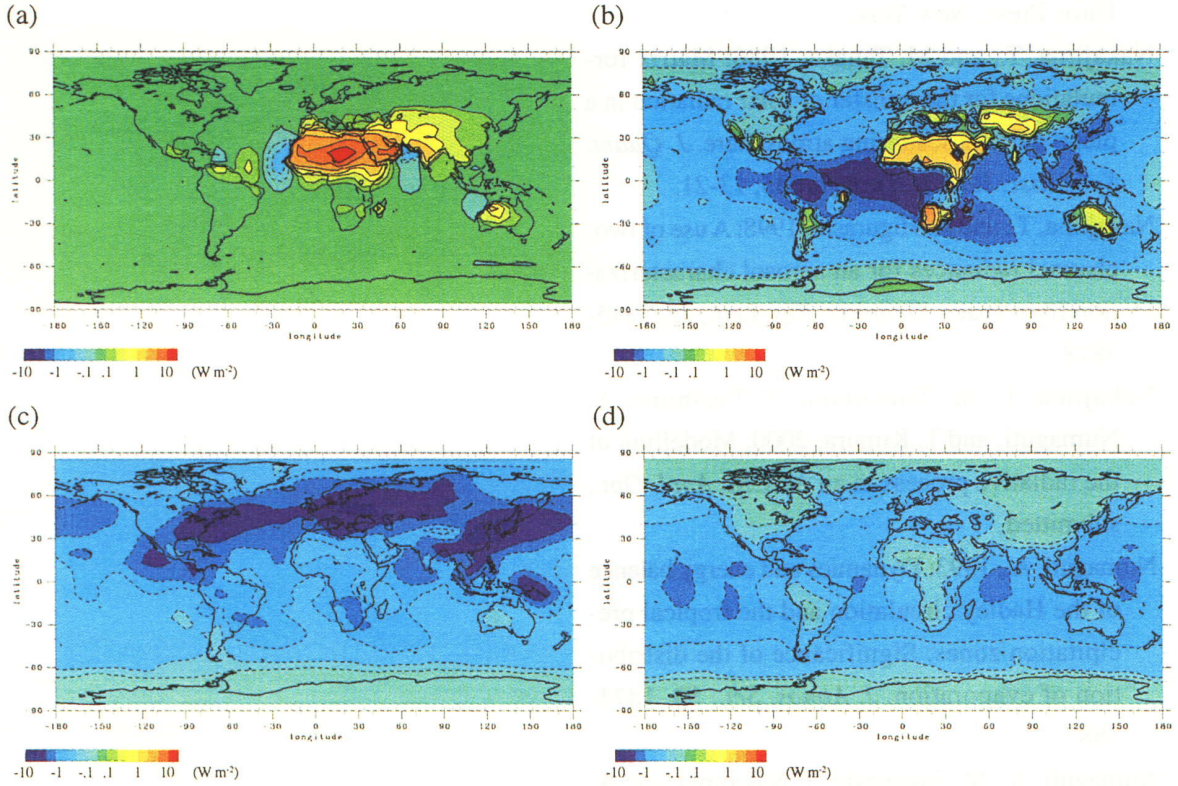

Figure 5. Annual mean aerosol direct forcing of net radiation at the tropopause for (a) soil dust, (b) carbonaceous, (c) sulfate, and (d) sea-salt aerosols for clear-sky in W m^{-2}.

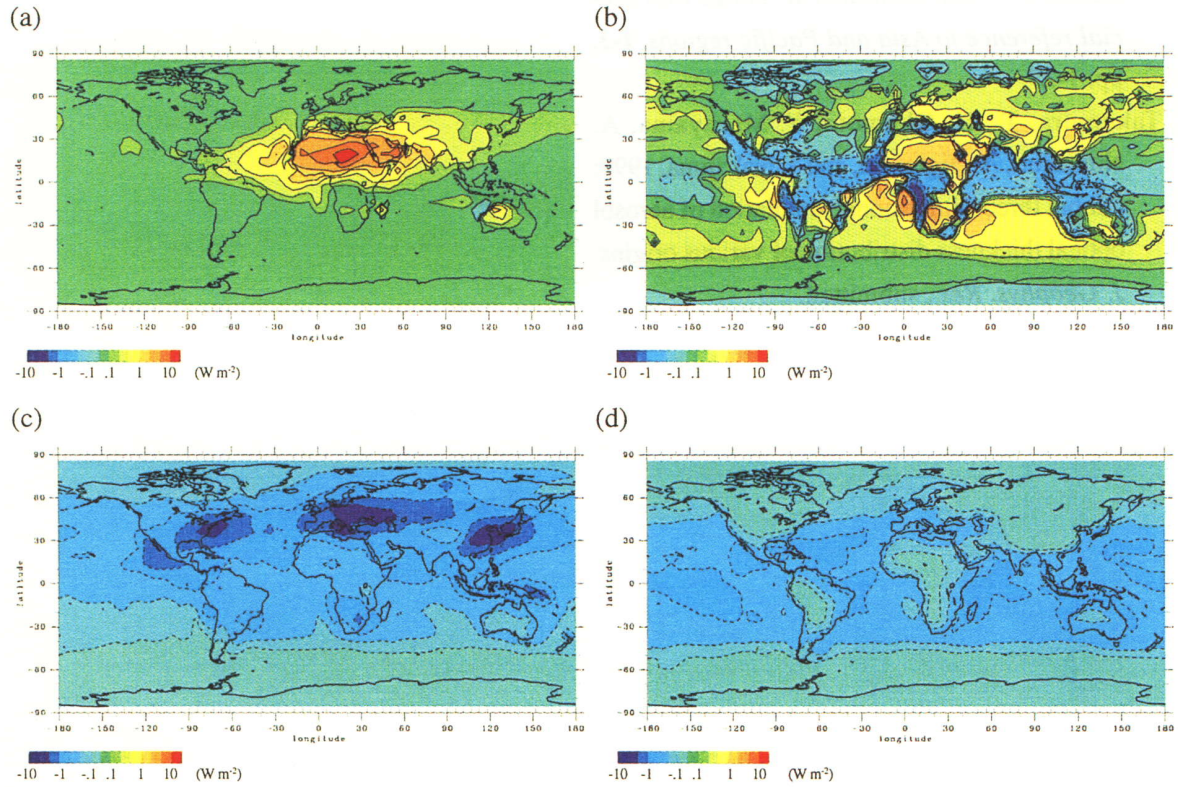

Figure 6. Sama as Figure 5 but for whole-sky.

Univ. Press, New York.

Nakajima, T., and M. Tanaka, 1986: Matrix formulations for the transfer of solar radiation in a plane-parallel scattering atmosphere. *J. Quant. Spectrosc. Radiat. Transfer*, **35**, 13-21.

Nakajima, T., and A. Higurashi, 1998: A use of two-channel radiances for an aerosol characterization from space. *Geophys. Res. Lett.*, **25**, 3815-3818.

Nakajima, T., M. Tsukamoto, Y. Tsushima, A. Numaguti, and T. Kimura, 2000: Modelling of the radiative process in an AGCM. *Appl. Opt.*, submitted.

Numaguti, A., 1993: Dynamics and energy balance of the Hadley circulation and the tropical precipitation zones: Significance of the distribution of evaporation. *J. Atmos. Sci.*, **50**, 1874-1887.

Numaguti, A., M. Takahashi, T. Nakajima, and A. Sumi, 1995: Development of an atmospheric general circulation model. in *Reports of a new program for creative basic research studies, Studies of global environment change with special reference to Asia and Pacific regions*, **I-3**, pp. 1-27.

Takemura, T., H. Okamoto, Y. Maruyama, A. Numaguti, A. Higurashi, and T. Nakajima, 1999: Global three-dimensional simulation of aerosol optical thickness distribution of various origins. *J. Geophys. Res.*, submitted.